

Floquet topological phase transition in two-dimensional quadratic band crossing system

Guo-Bao Zhu(朱国宝) and Hui-Min Yang(杨慧敏)

Citation: Chin. Phys. B, 2021, 30 (**6**): 067304. DOI: 10.1088/1674-1056/abdda4
Journal homepage: http://cpb.iphy.ac.cn; http://iopscience.iop.org/cpb

What follows is a list of articles you may be interested in

Tunable metal-insulator transition in $LaTiO_3/CaVO_3$ superlattices: A theoretical study

Ya-Kui Weng(翁亚奎), Meng-Lan Shen(沈梦兰), Jie Li(李杰), and Xing-Ao Li(李兴鳌)
Chin. Phys. B, 2020, 29 (12): 127303. DOI: 10.1088/1674-1056/abc237

Quantization of electromagnetic modes and angular momentum on plasmonic nanowires

Guodong Zhu(朱国栋), Yangzhe Guo(郭杨喆), Bin Dong(董斌), Yurui Fang(方蔚瑞)
Chin. Phys. B, 2020, 29 (**8**): 087301. DOI: 10.1088/1674-1056/ab9698

Optical spin-to-orbital angular momentum conversion instructured optical fields

Yang Zhao(赵阳), Cheng-Xi Yang(阳成熙), Jia-Xi Zhu(朱家玺), Feng Lin(林峰), Zhe-Yu Fang(方哲宇), Xing Zhu(朱星)
Chin. Phys. B, 2020, 29 (**6**): 067301. DOI: 10.1088/1674-1056/ab862a

Seeing Dirac electrons and heavy fermions in new boron nitride monolayers

Yu-Jiao Kang(康玉娇), Yuan-Ping Chen(陈元平), Jia-Ren Yuan(袁加仁), Xiao-Hong Yan(颜晓红), Yue-E Xie(谢月娥)
Chin. Phys. B, 2020, 29 (**5**): 057303. DOI: 10.1088/1674-1056/ab7e9e

Selective excitation of multipolar surface plasmon in a graphene-coated dielectric particle by Laguerre Gaussian beam

Yang Yang(杨阳), Guanghua Zhang(张光华), Xiaoyu Dai(戴小玉)
Chin. Phys. B, 2020, 29 (**5**): 057302. DOI: 10.1088/1674-1056/ab7e97

Floquet topological phase transition in two-dimensional quadratic band crossing system*

Guo-Bao Zhu(朱国宝) and Hui-Min Yang(杨慧敏)†

School of Physics and Electronic Engineering, Heze University, Heze 274015, *China*

(Received 2 November 2020; revised manuscript received 11 January 2021; accepted manuscript online 20 January 2021)

We investigate the Hall effects of quadratic band crossing (QBC) fermions in a square optical lattice with spin–orbit coupling and orbital Zeeman term. We find that the orbital Zeeman term and shaking play critical roles in the systems, which can drive a topological transition from spin Hall phases to anomalous Hall phase with nonvanishing (spin) Chern numbers. Due to the interplay among the orbital Zeeman term, spin–orbit coupling, and the shaking, the phase diagram of the system exhibits rich phases, which are characterized by Chern number.

Keywords: shaking, quadratic band crossing, orbital

PACS: 73.43.Nq, 37.10.Jk, 71.10.Fd **DOI:** 10.1088/1674-1056/abdda4

1. Introduction

Topological phases and phase transitions have become the subject of tremendous interest over the last decade.[1–3] In two-dimensional (2D) systems, topological insulating phases can be understood as generalizations of the quantum Hall effect. The quantum anomalous Hall effect[4] and the quantum spin Hall effect[5] have been predicted and intensively studied.[6,7]

On the other hand, ultracold atoms in optical lattices provide a clean and well-controllable platform to engineer the Hall effect.[8–15] For example, Goldman *et al.*[8] have shown a remarkable anomalous quantum Hall effect with an ultracold Fermi gas loaded in an optical square lattice and subjected to an external and classical non-Abelian gauge field. Kennedy *et al.*[9] have proposed a scheme to realize the quantum spin Hall effect for neutral atoms in optical lattices. Fractional quantum Hall states of dipolar fermions have been studied in a strained optical lattice.[11] Li *et al.*[13] studied the tunable quantum Hall effects in a non-Abelian honeycomb optical lattice. Phuc *et al.*[14] proposed a many-body spin Hall effect induced by the dipole–dipole interaction.

Moreover, time-periodic driving can be a powerful tool for manipulating quantum states in an optical lattice. In systems of ultracold atoms in optical lattices, Floquet modulation can be used to simulate anomalous quantum Hall phases and analog of topological insulators.[16] In a two-dimensional honeycomb lattice, the quantum anomalous Hall effect can be achieved by shaking optical lattices.[17,18] Mei *et al.*[19] have proposed the method to simulate and detect topological insulators with cold atoms trapped in a one-dimensional bichromatic optical lattice subjected to a time-periodic modulation. Furthermore, time-periodic modulations were used to study the topology properties of interacting fermionic atoms in shaken square optical lattices.[20,21] A periodic driving protocol was proposed to engineer large-Chern-number phases with the quantum anomalous Hall effect in a periodically shaken optical dice model.[22]

Given this background, we study quadratic band crossing (QBC) fermions in a square optical lattice, which have attracted intensive studies in modern condensed matter physics.[23–28] We find that the interplay between the shaking, orbital Zeeman term, and the spin–orbit coupling can lead to the nontrivial topology characterized by the (spin) Chern number of its energy band. By varying the orbital Zeeman term and shaking strength, the quantum spin Hall (QSH) and quantum anomalous Hall (QAH) phase may appear. Our findings would provide a way to study the topological physics of QBC fermions.

This paper is organized as follows. We first present the model Hamiltonian, including the scheme of shaking, orbital Zeeman term, and the spin–orbit coupling in Section 2. In Section 3, we analyze band structures. Based on these results, we further obtain the phase diagram of Hall phases in Section 4. Finally, in Section 5, we give a brief conclusion.

2. Model and method

We use the following low-energy effective Hamiltonian to describe QBC fermions in a square optical lattice

$$H = H_0 + H_{\rm SOC} + H_{\rm L}, \tag{1}$$

where

$$H_0 = t_I k^2 + 2t_x k_x k_y \sigma^x + t_z (k_x^2 - k_y^2)\sigma^z. \tag{2}$$

Here $t_{I,x,z}$ are determined by the hopping between orbitals on neighboring sites in a square optical lattice, and $\sigma^{x,y,z}$ are cor-

*Project supported by the National Natural Science Foundation of China (Grant No. 11504095).

†Corresponding author. E-mail: yangyhm@163.com

© 2021 Chinese Physical Society and IOP Publishing Ltd

responding Pauli matrices in the p_{xy}-orbital space[29] (see appendix A for details). The second part is the spin–orbit coupling (SOC), which is modeled as[30–32]

$$H_{\rm SOC} = s\lambda\sigma^y, \tag{3}$$

where λ is the spin–orbit coupling (SOC) strength, and $s = \pm$ are the spin index for the spin up and down bands. In optical lattice, SOC is experimentally realized via the Raman technique.[33–36] The last term is orbital Zeeman term from the on-site rotation by rotating each optical lattice site around its own center,[37] and is described by[38,39]

$$H_{\rm L} = V\sigma^y. \tag{4}$$

The last two terms break the time-reversal symmetry and induce topologically nontrivial band structures. t_x is taken as the unit of the parameters.

For a shaken optical lattice, the vector potential coming from shaking has the form[21]

$$A(t) = A_0[\cos\omega t, \cos(\omega t + \vartheta)], \tag{5}$$

where $A_0 = \omega s_0 k_{\rm L}/E_{\rm R}$ is the dimensionless shaking strength, and $k_{\rm L}$ and $E_{\rm R}$ are recoil momentum and recoil energy, respectively. In the practical experiment, weak lattice shaking is preferred to make induced heating on the lattice small. Then the above time-dependent Hamiltonian can be captured by an effective time-independent Hamiltonian as[19,40,41]

$$H^{\rm F}_{\rm eff} = H + \frac{[H_{-1}, H_1]}{\hbar\omega} + \frac{[H_{-2}, H_2]}{2\hbar\omega}, \tag{6}$$

where

$$H_{\pm m} = \frac{\omega}{2\pi}\int_0^{\frac{2\pi}{\omega}} H(t)\,{\rm e}^{\pm m{\rm i}\omega t}. \tag{7}$$

Straightforward calculations show

$$H^{\rm F}_{\rm eff} = H_0 + [s\lambda - V - \eta V_\omega]\,\sigma_y, \tag{8}$$

where

$$V_\omega = \frac{2t_x t_z}{\hbar\omega}\left(\frac{eA}{\hbar}\right)^2\left[2k^2 + \frac{1}{4}\left(\frac{eA}{\hbar}\right)^2\right], \tag{9}$$

and $\eta = \pm 1$ denote the circularity of shaking, which correspond to the $\vartheta = \mp\pi/2$, respectively. Based on the above equations, we can obtain that the shaking induced SOC-like term is introduced, and its sign depends on the circularity of shaking.

3. Band structure

Diagonalizing Eq. (6), we obtain the energy dispersion

$$E^{1,2} = (-1)^{1,2}\sqrt{4t_x^2k_x^2k_y^2 + t_z^2(k_x^2 - k_y^2)^2 + \Delta_\omega^2} + t_I k^2, \tag{10}$$

where $\Delta_\omega = s\lambda - V - V_\omega\eta$. The parameters $t_{I,x,z}$ can be controlled by the over-lap between orbital on neighboring sites. It should be noted that the term $t_I k^2$ does not modify the eigenstates and topological properties of the system. Therefore, we consider the system with $t_I = 0$.

Figures 1 and 2 show the evolution of the energy band near QBC point along with the increase of a shaking strength at circularity of shaking $\eta = -1$ and $t_x = t_z$ at $\lambda = 0.05t_x$, $V = 0.1t_x$ and $\lambda = 0.05t_x$, $V = 0.01t_x$, respectively. When the shaking is present, a bulk gap is opened due to SOC and V, and the four bands are nondegenerate. For $\lambda < V$, the band gap of spin-up ($s = 1$) bands firstly closes and then reopens with the increase of a shaking strength. With the further increase of a shaking strength, the band gap of spin-down ($s = -1$) bands closes and then reopens. For $\lambda > V$, the band gap of spin-down bands closes and reopens, while the band gap of spin-up bands always increases. This band structure is drastically modified by shaking; the rich change of band gaps in the system is shown in Fig. 3 under the interplay between SOC, V, and shaking. Moreover, the presence of such a bulk gap indicates an insulating state. The quantum Hall effect can be engineered by opening a gap at a topological Fermi point with a quadratic band dispersion. As a consequence, the band topologies may get changed with the evolution of the band gap, and interesting topological transitions occur. As we argue below, this insulating state is topologically nontrivial and exhibiting a quantized Hall conductance.

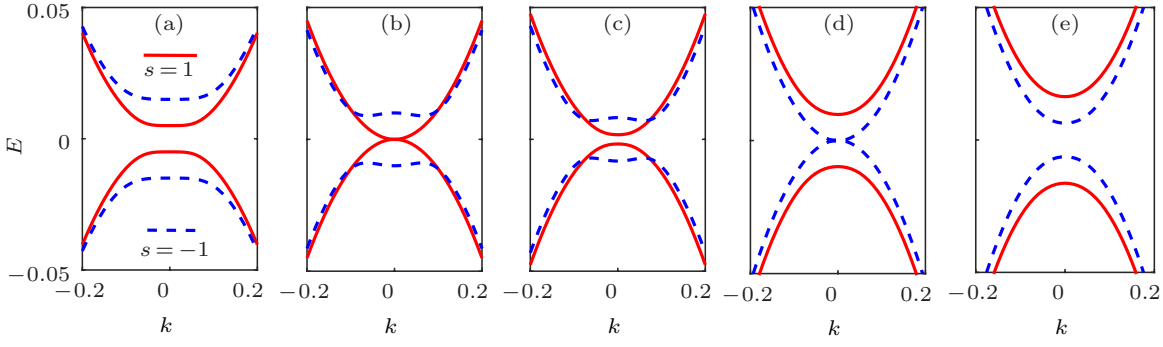


Fig. 1. Band structures near quadratic band crossing (QBC) point under the circularity of shaking $\eta = -1$ at $\lambda = 0.05t_x$, $V = 0.1t_x$, and $t_I = 0$ for a shaking strength A_0 of (a) 0, (b) 0.278, (c) 0.3, (d) 0.365, (e) 0.4, respectively. The solid red and dashed blue lines denote spin-up ($s = 1$) and spin-down ($s = -1$) bands, respectively.

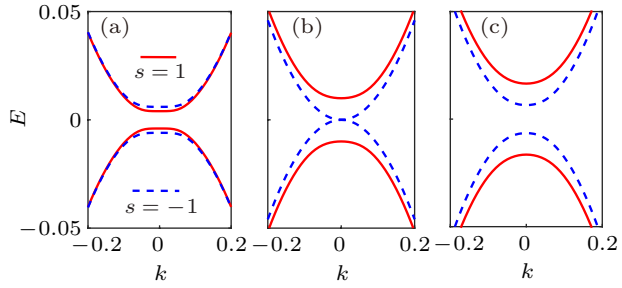


Fig. 2. Band structures near QBC point under the circularity of shaking $\eta=-1$ at $\lambda=0.05t_x$, $V=0.01t_x$, and $t_I=0$ for a shaking strength A_0 of (a) 0, (b) 0.291, (c) 0.35, respectively. The solid red and dashed blue lines denote spin-up ($s=1$) and spin-down ($s=-1$) bands, respectively.

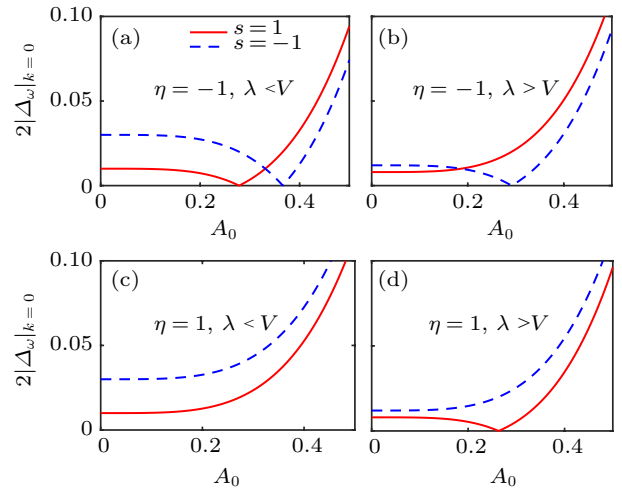


Fig. 3. Band gap ($2|\Delta_\omega|_{k=0}$) as a function of the shaking strength A_0 for (a) $\eta=-1,\lambda<V$, (b) $\eta=-1,\lambda>V$, (c) $\eta=1,\lambda<V$, and (d) $\eta=1,\lambda>V$. The solid red and dashed blue lines denote spin-up ($s=1$) and spin-down ($s=-1$) bands, respectively.

4. Phase diagram

For two dimensional system, the Hamiltonian can be expressed in terms of the Pauli matrices as

$$H(k)=d(k)\cdot\hat{\sigma}+d_0(k)\boldsymbol{I}, \tag{11}$$

where $d(k)=(d_x(k),d_y(k),d_z(k))$, $\hat{\sigma}=(\sigma_x,\sigma_y,\sigma_z)$, and $\boldsymbol{I}$ is 2×2 identity matrix. Then, due to the good quantum numbers of spin, the corresponding Chern number for spin s component is calculated as[42]

$$N_s=\frac{1}{2\pi}\int \mathrm{d}^2\boldsymbol{k}\Omega_s(\boldsymbol{k}), \tag{12}$$

where Ω_s is the Berry curvature of spin s component in the momentum space over all occupied states, and it can be written as

$$\Omega_s(\boldsymbol{k})=\frac{1}{2}\hat{d}\cdot\left(\frac{\partial\hat{d}}{\partial k_x}\times\frac{\partial\hat{d}}{\partial k_y}\right), \tag{13}$$

where $\hat{d}=d/|d|$. Straightforward calculation shows

$$\Omega_s(\boldsymbol{k})=\frac{2t_xt_zk^2\left[s\lambda-V-\eta\dfrac{t_xt_z}{2\hbar\omega}\left(\dfrac{eA_0}{\hbar}\right)^4\right]}{\left[4t_x^2k_x^2k_y^2+t_z^2(k_x^2-k_y^2)^2+(s\lambda-V-\eta V_\omega)^2\right]^{3/2}}, \tag{14}$$

$$N_s=\mathrm{sgn}(s\lambda-V-\eta V_\omega)|_{k=0}, \tag{15}$$

where sgn is the sign function.

The total Chern number $C=N_++N_-$ indicates that the system exhibits QAHE, and the spin-Chern number $C_s=\frac{1}{2}(N_+-N_-)$ indicates that the system exhibits QSHE. In Fig. 4, we plot a phase diagram in (A_0,V) plane at fixed $\lambda=0.05t_x$ for circularity of shaking (a) $\eta=-1$ and (b) $\eta=1$. Figure 4 clearly shows that there are two QAH phases with $C=\pm2$, and one QSH phase with $C_s=1$. By tuning V and shaking strength A_0, the system would undergo the transitions between these phases. When the shaking is absent ($A_0=0$), the system is in QAH (QSH) phase for $\lambda<V$ ($\lambda>V$). For $\lambda<V$, an exotic QAH–QSH–QAH phase transition is driven by increasing A_0 from 0 for circularity of shaking $\eta=-1$, while there is no topological phase transition for circularity of shaking $\eta=1$. For $\lambda>V$, a topological phase transition between QSH and QAH phase occurs along with the increase of A_0 for the two circularity of shaking.

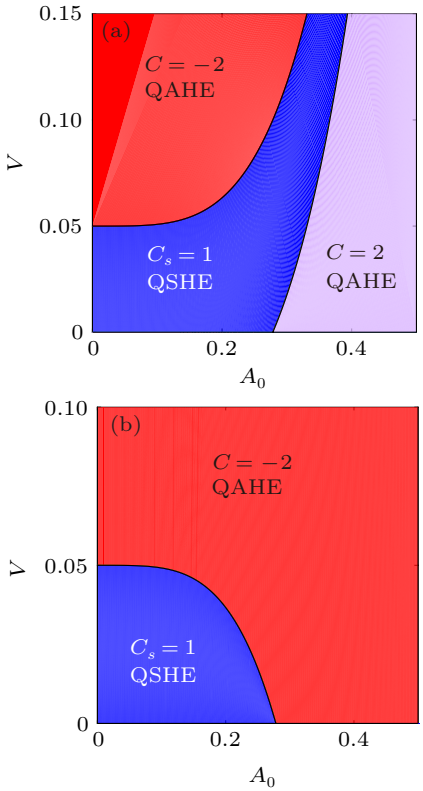


Fig. 4. Phase diagram in the (A_0,V) plane at fixed $\lambda=0.05$ for circularity of shaking (a) $\eta=-1$ and (b) $\eta=1$. There are two QAH phases, which are identical Chern number $C=2$ and $C=-2$, respectively. The other phase is QSH phase with spin Chern number $C_s=1$.

In addition to Chern number and spin Chern number, we discuss the energy gaps, which provide a more intuitive picture to characterize the topological phase transition. A topological phase transition occurs when the energy gap closes and reopens. In Fig. 3, we plot the band gap evolution as a function of shaking strength A_0. For $\lambda<V$, we find that the band gaps always open for $\eta=1$, while the process of band gap closing

and reopening occurs twice for $\eta = -1$. It means that there are two or no topological phase transitions along with the increase of shaking strength depending on the circularity of shaking. For $\lambda > V$, one can observe that the band gap of spin-up or spin-down bands opens and reopens, which is independent of the circularity of shaking. It indicates that a topological phase transition occurs.

The appearance of the edge state is another hallmark QAHE state. As an example, Fig. 5 shows the band structure of a ribbon under the shaking $\eta = -1$ at $\lambda = 0.05t_x$, $V = 0.01t_x$, and $t_I = 0$ for open boundary condition in the x direction without (a) and with (b) the shaking driving. When the shaking driving is absent, the edge state does not exist for a given Fermi level ($E_F = 0$). While there are four different edge states when the shaking driving is included. The emergence of edge states in the gap is intimately related to the topological property of the Bloch states in the valence bands. The numbers of edge states are in agreement with the Chern number.

Moreover, many techniques have been implemented to detect QAH and QSH states in the optical lattice in the experiment. Chiral edge states and topological order are hallmarks of quantum Hall physics. Alba *et al.*[43] provided the time-of-flight imaging methodology through measuring atomic distribution in momentum space. By performing Bloch oscillations,[40,44] an experimental value for the Chern number has been obtained. Using atomic interferometry in real and momentum space,[45–47] topological invariants of topological band structures in the optical lattice can be measured. By imaging individual sites along a synthetic dimension, Goldman *et al.*[48] have reported on the experimental realization of chiral edge states, which are hallmarks of quantum Hall physics.

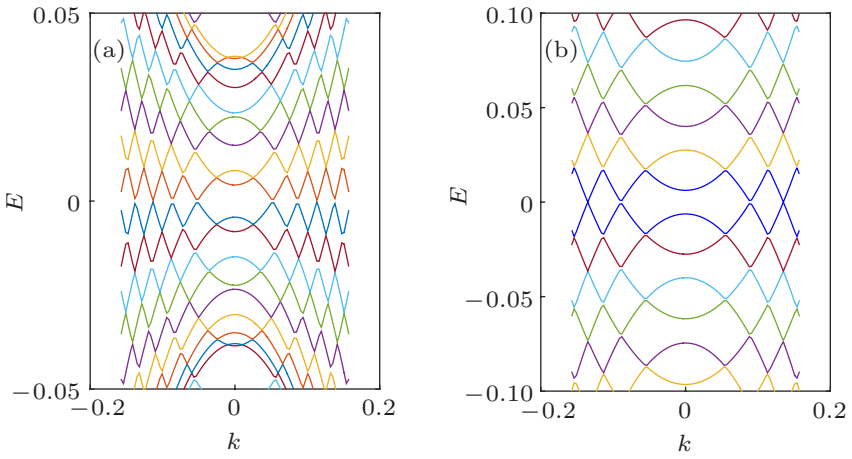


Fig. 5. Band structure of a ribbon under the shaking $\eta = -1$ at $\lambda = 0.05t_x$, $V = 0.01t_x$, and $t_I = 0$ before and after closing the gap with a shaking strength of (a) 0.2 and (b) 0.4, respectively.

5. Conclusion

We have studied the Hall effects of quadratic band crossing (QBC) fermions in a square optical lattice with spin–orbit coupling and orbital Zeeman term. By analyzing the energy gap and (spin) Chern numbers, we find that the orbital Zeeman term or shaking can drive a topological transition from spin Hall phases to anomalous Hall phase. The orbital Zeeman term can interplay with spin–orbit coupling and the shaking, and leads to rich phases. Our results provide a way to study the topological physics of spin–orbit coupling or shaking-driven topological phase.

Appendix A: Effective Hamiltonian

We consider ultracold fermionic atoms trapped in a square optical lattice with orbitals (p_x, p_y, and d). We assume that all the atoms are trapped in the lowest band of the optical lattice. Using perturbation theory,[29,49] one can get the tight-binding Hamiltonian in momentum space on the basis of $\{p_x(\boldsymbol{k}), p_y(\boldsymbol{k})\}$

$$H_{\boldsymbol{k}} = h_0 + 2t_x \sin k_x \sin k_y \sigma^x + h_z \sigma^z, \tag{A1}$$

where $h_0 = t_{pp}\cos k_x - t'_{pp}\cos k_y + t_{pp}\cos k_y - t'_{pp}\cos k_x + t_x \sin^2 k_x + t_x \sin^2 k_y$, $h_z = t_{pp}\cos k_x - t'_{pp}\cos k_y - t_{pp}\cos k_y + t'_{pp}\cos k_x + t_x \sin^2 k_x - t_x \sin^2 k_y$, and $t_x = 2t_{pd}^2/(2t_{pp} - 2t'_{pp} + 4t_{dd} - \delta)$. $t_{pp}, t'_{pp}, t_{dd}, t_{pd}$ are the hopping amplitudes between orbitals on neighboring sites, and δ describes the energy difference between p and d orbitals. To describe QBC fermions, we expand the momentum around the Γ point and obtain

$$H_0 = t_I k^2 + 2t_x k_x k_y \sigma^x + t_z(k_x^2 - k_y^2)\sigma^z,$$

with $t_I = t_{pp} - t'_{pp} + 2t_x$ and $t_z = t_{pp} + t'_{pp} + 2t_x$.

Based on Eq. (5), when the shaking is included, we can obtain

$$H_{F0}^{\mathrm{TB}} = h_0^{\mathrm{F}} + 2J_0(\sqrt{2}A_0)t_x \sin k_x \sin k_y \sigma^x + h_z^{\mathrm{F}}\sigma^z, \tag{A2}$$

with

$$h_0^{\mathrm{F}} = J_0(A_0)t_{pp}\cos k_x - J_0(A_0)t'_{pp}\cos k_y + J_0(A_0)t_{pp}\cos k_y - J_0(A_0)t'_{pp}\cos k_x + J_0(2A_0)t_x \sin^2 k_x + J_0(2A_0)t_x \sin^2 k_y,$$

$$
\begin{aligned}
h_z^{\mathrm{F}} &= J_0(A_0)t_{pp}\cos k_x - J_0(A_0)t'_{pp}\cos k_y - J_0(A_0)t_{pp}\cos k_y \\
&\quad + J_0(A_0)t'_{pp}\cos k_x + J_0(2A_0)t_x\sin^2 k_x - J_0(2A_0)t_x\sin^2 k_y;
\end{aligned}
$$

$$
H_{F\pm1}^{\mathrm{TB}} = h_{\pm1}^{\mathrm{F}} + h_{\pm1}^{\mathrm{F}}\sigma^z, \tag{A3}
$$

with

$$
\begin{aligned}
h_{\pm1}^{\mathrm{F}} &= -J_1(A_0)t_{pp}\sin k_x - \mathrm{i}J_{\pm1\eta}(A_0)t'_{pp}\sin k_y \\
&\quad + \mathrm{i}J_{\pm1\eta}(A_0)t_{pp}\sin k_y + J_1(A_0)t'_{pp}\sin k_x \\
&\quad + J_1(2A_0)t_x\cos(2k_x)/2 - \mathrm{i}J_{\pm1\eta}(2A_0)t_x\sin(2k_y)/2, \\
h_{\pm1}^{\mathrm{F}} &= -J_1(A_0)t_{pp}\sin k_x - \mathrm{i}J_{\pm1\eta}(A_0)t'_{pp}\sin k_y \\
&\quad - \mathrm{i}J_{\pm1\eta}(A_0)t_{pp}\sin k_y - J_1(A_0)t'_{pp}\sin k_x \\
&\quad + J_1(2A_0)t_x\cos(2k_x)2 + \mathrm{i}J_{\pm1\eta}(2A_0)t_x\sin(2k_y)/2;
\end{aligned}
$$

$$
H_{F\pm2}^{\mathrm{TB}} = h_{\pm2}^{\mathrm{F}} + h_{\pm2}^{\mathrm{F}}\sigma^z, \tag{A4}
$$

with

$$
\begin{aligned}
h_{\pm2}^{\mathrm{F}} &= -J_2(A_0)t_{pp}\cos k_x - J_2(A_0)t'_{pp}\cos k_y + J_2(A_0)t_{pp}\cos k_y \\
&\quad + J_2(A_0)t'_{pp}\cos k_x + J_2(2A_0)t_x\cos(2k_x)/2 \\
&\quad - J_2(2A_0)t_x\cos(2k_y)/2, \\
h_{\pm2}^{\mathrm{F}} &= -J_2(A_0)t_{pp}\cos k_x - J_2(A_0)t'_{pp}\cos k_y - J_2(A_0)t_{pp}\cos k_y \\
&\quad - J_2(A_0)t'_{pp}\cos k_x + J_2(2A_0)t_x\cos(2k_x)/2_x \\
&\quad + J_2(2A_0)t_x\cos(2k_x)/2.
\end{aligned}
$$

References

[1] Ren Y, Qiao Z and Niu Q 2016 *Rep. Prog. Phys.* **79** 066501
[2] Hasan M Z and Kane C L 2010 *Rev. Mod. Phys.* **82** 3045
[3] Qi X L and Zhang S C 2011 *Rev. Mod. Phys.* **83** 1057
[4] Haldane F D M 1988 *Phys. Rev. Lett.* **61** 2015
[5] Kane C L and Mele E J 2005 *Phys. Rev. Lett.* **95** 146802
[6] Nagaosa N, Sinova J, Onoda S, MacDonald A H and Ong N P 2010 *Rev. Mod. Phys.* **83** 1539
[7] Sinova J, Valenzuela S O, Wunderlich J, Back C H and Jungwirth T 2015 *Rev. Mod. Phys.* **87** 1213
[8] Goldman N, Kubasiak A, Bermudez A, Gaspard P, Lewenstein M and Martin-Delgado M A 2009 *Phys. Rev. Lett.* **103** 035301
[9] Kennedy C J, Siviloglou G A, Miyake H, Burton W C and Ketterle W 2013 *Phys. Rev. Lett.* **111** 225301
[10] Stuhl B K, Lu H I, Aycock L M, Genkina D and Spielman I B 2015 *Science* **349** 1514
[11] Fujita H, Nakagawa Y O, Ashida Y and Furukawa S 2016 *Phys. Rev. A* **94** 043641
[12] Ghosh S K, Greschner S, Yadav U K, Mishra T, Rizzi M and Shenoy V B 2017 *Phys. Rev. A* **95** 063612
[13] Li L, Hao N, Liu G, Bai Z, Li Z D, Chen S and Liu W M 2015 *Phys. Rev. A* **92** 063618
[14] Phuc N T and Ueda M 2018 *Phys. Rev. A* **97** 061608
[15] Görg F, Messer M, Sandholzer K, Jotzu G, Desbuquois R and Esslinger T 2018 *Nature* **553** 481
[16] Plekhanov K, Roux G and Le Hur K 2017 *Phys. Rev. B* **95** 045102
[17] Zheng W and Zhai H 2014 *Phys. Rev. A* **89** 061603
[18] Verdeny A and Mintert F 2015 *Phys. Rev. A* **92** 063615
[19] Mei F, You J B, Zhang D W, Yang X C, Fazio R, Zhu S L and Kwek L C 2014 *Phys. Rev. A* **90** 063638
[20] Račiūnas M, Žlabys G, Eckardt A and Anisimovas E 2016 *Phys. Rev. A* **93** 043618
[21] Keleş A, Zhao E and Liu W V 2017 *Phys. Rev. A* **95** 063619
[22] Cheng S, Yin H, Lu Z, He C, Wang P and Gao X 2020 *Phys. Rev. A* **101** 043620
[23] Sun K, Yao H, Fradkin E and Kivelson S 2009 *Phys. Rev. Lett.* **103** 046811
[24] Moon E G 2012 *Phys. Rev. B* **85** 245123
[25] Chern G W and Batista C D 2012 *Phys. Rev. Lett.* **109** 156801
[26] Murray J M and Vafek O 2014 *Phys. Rev. B* **89** 201110
[27] Pawlak K A, Murray J M and Vafek O 2015 *Phys. Rev. B* **91** 134509
[28] Dóra B and Herbut I F 2016 *Phys. Rev. B* **94** 155134
[29] Sun K, Liu W V, Hemmerich A and Das Sarma S 2012 *Nat. Phys.* **8** 67
[30] Zhang G F, Li Y and Wu C 2014 *Phys. Rev. B* **90** 075114
[31] Huang H and Liu F 2018 *Phys. Rev. Lett.* **121** 126401
[32] Amin V P, Li J, Stiles M D and Haney P M 2019 *Phys. Rev. B* **99** 220405
[33] Galitski V and Spielman I B 2013 *Nature* **4** 49
[34] Zhai H 2015 *Rep. Prog. Phys.* **78** 026001
[35] Zhang Y, Mossman M E, Busch T, Engels P and Zhang C 2016 *Front. Phys.* **11** 118103
[36] Wang Y Q and Zhang C 2017 arXiv:2017.02070 [cond-mat]
[37] Gemelke N 2007 *Quantum Degenerate Atomic Gases in Controlled Optical Lattice Potentials* (Ph. D. Dissertation) (Stanford University)
[38] Wu C 2008 *Phys. Rev. Lett.* **101** 0186807
[39] Zhang M, Hung H H, Zhang C and Wu C 2011 *Phys. Rev. A* **83** 023615
[40] Jotzu G, Messer M, Desbuquois R, Lebrat M, Uehlinger T, Greif D and Esslinger T 2014 *Nature* **515** 237
[41] Goldman N and Dalibard J 2014 *Phys. Rev. X* **4** 031027
[42] Qi X L, Hughes T L and Zhang S C 2008 *Phys. Rev. B* **78** 195424
[43] Alba E, Fernandez-Gonzalvo X, Mur-Petit J, Pachos J K and Garcia-Ripoll J J 2011 *Phys. Rev. Lett.* **107** 235301
[44] Aidelsburger M, Lohse M, Schweizer C, Atala M, Barreiro J, Nascimbène S, Cooper N, Bloch I and Goldman N 2014 *Nat. Phys.* **11** 162
[45] Abanin D A, Kitagawa T, Bloch I and Demler E 2013 *Phys. Rev. Lett.* **110** 165304
[46] Atala M, Aidelsburger M, Barreiro J T, Abanin D, Kitagawa T, Demler E and Bloch I 2013 *Nat. Phys.* **9** 795
[47] Duca L, Li T, Reitter M, Bloch I, Schleier-Smith M and Schneider U 2015 *Science* **347** 288
[48] Mancini M, Pagano G, Cappellini G, Livi L, Rider M, Catani J, Sias C, Zoller P, Inguscio M, Dalmonte M, and Fallani L 2015 *Science* **349** 1510
[49] Liu C C, Jiang H and Yao Y 2011 *Phys. Rev. B* **84** 195430